Enhancement of Fine-Scale Turbulence for Improving Fuel-Rich Plume Combustion

K. C. Schadow,* E. Gutmark,† T. P. Parr,‡ D. M. Parr‡, and K. J. Wilson§
Naval Weapons Center, China Lake, California
and
G. B. Ferrell¶
Texas Technical University, Lubbock, Texas

A passive method to enhance fine-scale mixing was developed and studied in cold flows. Its effect on the combustion intensity and flame stability was then studied in reacting flows. Hot-wire anemometry was used to map the mean and turbulent flowfields of the nonreacting flows. Reacting flows were studied in a free flame and ducted gas-generator fuel-rich plume using planar laser-induced fluorescence imaging, a rake of thermocouples, and high-speed photography. A modified circular nozzle having several downstream-facing steps upstream of its exit was used to introduce numerous inflection points in the initial mean velocity profiles, thus producing multiple corresponding sources of fine-scale turbulence generators and reducing the strain rates in the initial region. Cold flow tests showed turbulence increases of up to six times the initial turbulence level relative to a circular nozzle and a substantial decrease of the mean velocity gradient. The flame of this nozzle was more intense with a homogeneous heat release in the free-flame experiments and ducted-plume combustion experiments, even when the gas-generator exhaust velocity was supersonic. Secondary plume ignition was obtained under conditions that prevented sustained afterburning using the circular nozzle.

Nomenclature

D	= jet nozzle diameter
D_C	= diameter of duct (ducted-jet tests)
D_{CH}	= diameter of secondary chamber (ducted-plume tests)
D_t	= secondary-chamber-exit nozzle diameter
f	= frequency
f_F	= forcing frequency
f_j	= dominant frequency of the velocity fluctuations spectrum at the end of the jet's potential core
$(L/H)_{ST}$	= length-to-step height ratio in multistep nozzle
$\dot{m}_A$	= air-mass flow
$\dot{m}_{CH}$	= ethylene-mass flow
$\dot{m}_N$	= nitrogen-mass flow
$\dot{m}_o$	= oxygen-mass flow
N_{ST}	= number of steps in multistep nozzle
P_C	= combustion pressure
P_{CH}	= chamber pressure
R	= jet nozzle radius ($=D/2$)
R_C	= radius of duct (ducted-jet tests)
R_{CH}	= radius of secondary chamber (ducted-plume tests)
$R_{0.5}$	= jet half-width based on mean velocity profile
$(R_{0.5})_0$	= jet half-width at $x = 0$
$R_{0.5T}$	= jet half-width based on temperature profile
r	= radial coordinate
St	= Strouhal number ($=f \cdot D/u$)
St_j	= jet-preferred-mode Strouhal number ($St_j = f_j \cdot D/u$)
T	= combustion temperature
T_0	= temperature at gas-generator exit
U_{CL}	= centerline velocity
U_0	= velocity at $x = 0$
u	= mean velocity
u'	= velocity fluctuations
x	= axial distance from nozzle exit
ΔP	= peak-to-peak oscillating-pressure amplitude
ϕ	= equivalence ratio
ν	= kinematic viscosity

Introduction

AFTERBURNING of fuel-rich reaction products in air is relevant to problems in many propulsion systems. To achieve high reaction rates (specifically for the particulate fuels, such as soot particles), it is important to achieve the highest local combustion temperatures possible. For combustion (afterburning) of fuel-rich gas-generator reaction products in a coaxial airstream, the highest local theoretical combustion temperatures associated with near-stoichiometric mixture ratios exist in the extreme fore-end of the mixing region near the gas-generator nozzle (Fig. 1). These theoretical temperatures were computed based on experimental mixture ratios.[1] To realize the high local combustion temperatures, it is necessary to initiate combustion in the mixing regions near the nozzle, which, however, has been difficult to achieve, especially when the gas-generator exhaust was supersonic and the afterburning occurred at low pressure.[2,3] The probable cause of lack of combustion near the gas-generator nozzle was the effect of turbulence on combustion or limited fine-scale mixing in the presence of large-scale vortices, in addition to the high strain rates due to high-velocity gradients that characterize a high-speed reacting jet approaching flame liftoff or blowout.[4,5]

Recent developments in the understanding of the important role of large-scale coherent structures in shear-layer dynamics[6,7] opened up the possibility to modify the regular break-

Received April 27, 1987; revision received Oct. 15, 1987.

*Supervisory General Engineer.
†Aerospace Engineer. Member AIAA.
‡Research Chemist.
§Aerospace Engineer.
¶Assistant Professor.

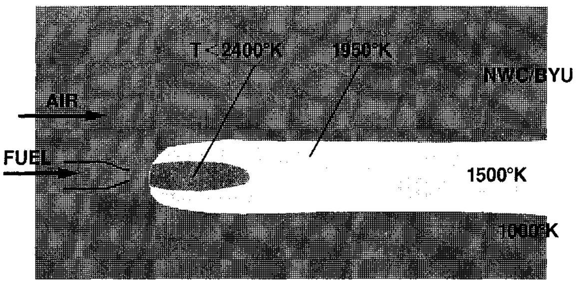

Fig. 1 Theoretical gas-phase combustion temperature based on experimental mixture ratios.

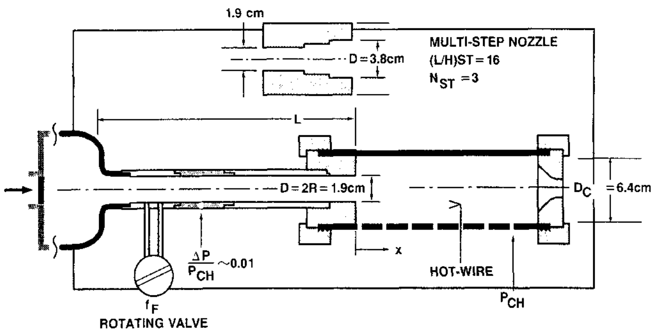

Fig. 2 Experimental setup: ducted jet with circular and multistep nozzles.

down of large-scale vortices into fine-scale turbulence and, therefore, to enhance molecular mixing and reduce strain rates as necessary for combustion to occur. Augmentation of fine-scale mixing and afterburning of fuel-rich, gas-generator reaction products has been achieved using elliptical gas-generator nozzles.[8] The improvements were due to the complex dynamics of the elliptical vortices formed as a result of the initial instability of the jet.[9]

In this paper, fine-scale turbulence enhancement is studied using an axisymmetric nozzle with a series of downstream-facing steps inside this "multistep nozzle." The idea is based on the theoretically proven relation between the number of unstable modes and inflection points in the velocity profile. This relation was described by Howard[10] and was shown to be valid for instability problems governed by the Rayleigh stability equations. The concept of the multistep nozzle, to enhance fine-scale mixing by increasing the number of sources for turbulence production, was investigated in nonreacting flows, annular diffusion flames before it was applied to afterburning of fuel-rich gas-generator reaction products in a coaxial airstream.

Experimental Setup

Three experimental setups were used to compare shear-flow and combustion characteristics between a circular and a multistep nozzle.

In the nonreacting ducted-jet setup schematically shown in Fig. 2, mean and fluctuating velocities were compared for a jet issued from a 50.8-cm long pipe with an inside diameter of $D = 1.9$ cm and a jet issued from a multistep nozzle having three downstream-facing steps ($N_{ST} = 3$), each with a length-to-step height ratio of $(L/H)_{ST} = 16$ and an exit diameter of 3.8 cm. For both nozzles, the mass-flow rate was held constant, resulting in identical flow conditions with $Re = U_0 \times D/\nu = 6.3 \times 10^4$ at the exit of the circular nozzle as well as at the entrance into the multistep section. The exit centerline velocity was $U_0 = 50$ m/s in both nozzles. This comparison between both nozzles at constant-mass flow and U_0 was preferred to a comparison at which the circular nozzle would have the same exit diameter at the multistep nozzle, because, for the latter case, it is impossible to maintain as constant both the exit velocity and the air-mass flow rate.

For the mean and fluctuating velocity measurements, the hot wire was mounted on a computer-controlled traverse mechanism. Calibration, data acquisition, and data reduction were done on a computer.

The ducted flow was forced at a desired frequency f_F and peak-to-peak pressure amplitude ΔP by exhausting a small amount of the inlet duct air through a rotating valve. Highest ΔP was achieved when f_F matched one of the resonant acoustic modes of the inlet duct. The experiments with the circular nozzle were performed at $f_F = 120$ Hz at which $\Delta P/P_{CH} \approx 0.01$ (where P_{CH} is the chamber pressure) was obtained. The corresponding Strouhal number was $St = f_F \times D/U_0 = 0.03$. The experiments with the multistep nozzle were performed at 85 Hz at which the maximum $\Delta P/P_{CH} \approx 0.01$ was achieved.

Subsequently, both nozzles were compared in a propane/air burner. The fuel was injected from the lip of the circular nozzle and the multistep nozzle [with $N_{ST} = 2$ and $(L/H)_{ST} = 5$] into the developing shear flow of an air jet with $Re = U_0 D/\nu = 7000$ to achieve an annular diffusion flame. The characteristics of the reacting shear flow were visualized by planar laser-induced fluorescence (PLIF) imaging of in-situ OH radicals. In this technique,[11,12] which is schematically shown in Fig. 3, an excimer laser beam was expanded into a thin sheet and excited OH molecules in the flame of the burner. The fluorescence was imaged with an intensified diode-array camera. Experiments with and without acoustic forcing via a loudspeaker in the plenum chamber were performed.

Finally, the circular and multistep nozzles were used at the outlet of a gas generator burning ethylene and oxygen at an equivalance ratio of $\phi = 2.46$ (Fig. 4). Nitrogen was added to reduce the gas-generator temperature to $T_C \approx 1700$ K. The circular nozzle diameter and multistep nozzle diameter upstream of the steps were $D = 1.9$ cm. The exit diameter of the multistep nozzle was 3.8 cm. A restriction (throat) of 0.54 D was located upstream of the nozzles, which caused a total

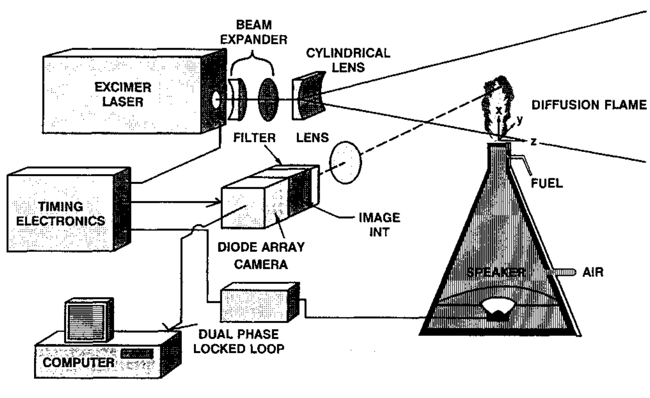

Fig. 3 Planar laser-induced fluorescence (PLIF) imaging setup.

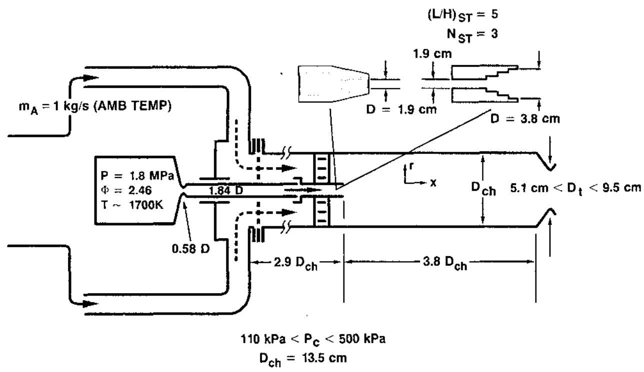

Fig. 4 Experimental setup: fuel-rich plume combustion using circular and multistep gas-generator nozzles.

pressure loss of an estimated 50% due to shock losses. The secondary-chamber (afterburner) pressure was changed between 100 kPa $< P_C <$ 500 kPa by varying the secondary-chamber throat diameter. It was estimated that for $P_C <$ 300 kPa, sonic speed was achieved at the gas-generator nozzle exit, as confirmed by the observation of Mach diamonds in photos of the plume at lower secondary-chamber pressures.

In these ducted-plume experiments, the afterburning characteristics of the fuel-rich gas-generator products in a coaxial airstream were compared for both nozzles using a rake of eight tungsten/rhenium thermocouples and direct high-speed color photography through a plexiglass-walled section of the secondary chamber.

Results and Discussion

Nonreacting Flow

The concept of enhancing fine-scale turbulence by introducing multiple inflection points into the shear-layer mean velocity profile was tested in a circular jet. Figure 5 compares the mean velocity profiles of a regular jet having one inflection point and a modified jet having two inflection points. The same figure shows the corresponding turbulence intensity. The regular jet has a typical single-peak distribution across the shear layer. The other jet has two peaks corresponding to two sources of instability in the jet shear layer.

This principle was extended by designing a nozzle with multiple downstream-facing steps. The small sequential shear layers, generated at each one of the steps, modified the mean velocity profile to include numerous inflection points, increase the momentum thickness, and decrease the radial gradient of the mean velocity without changing the centerline velocity of $U_0 = 50$ m/s (Fig. 6). All the modifications are expected to enhance combustion in the initial shear-flow regime. Although

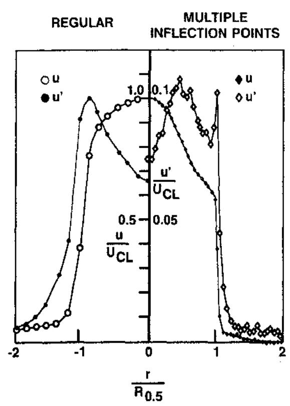

Fig. 5 Comparison of shear layers with regular shape and multiple inflection points.

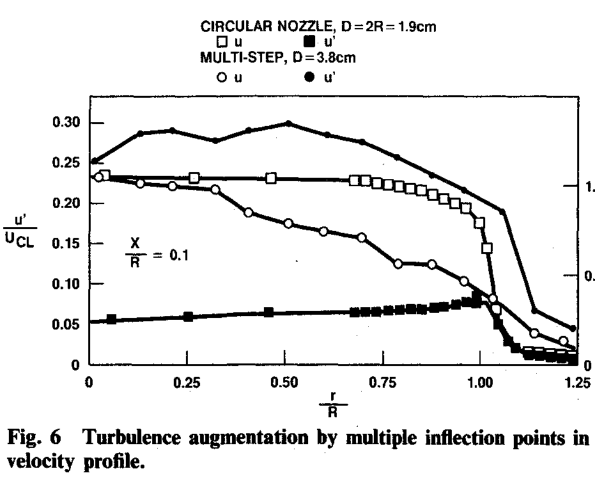

Fig. 6 Turbulence augmentation by multiple inflection points in mean velocity profile.

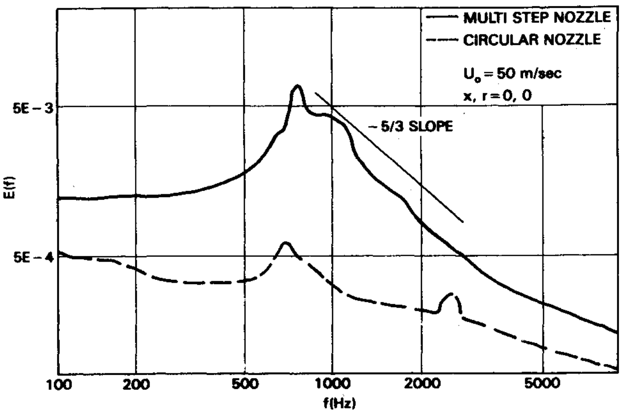

Fig. 7 Spectral distribution of turbulent fluctuations in the center of the exit plane of the multistep and circular jets.

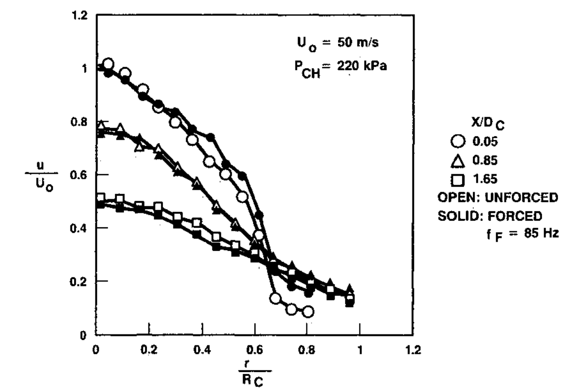

Fig. 8 Effect of forcing on ducted, multistep jet (mean velocity).

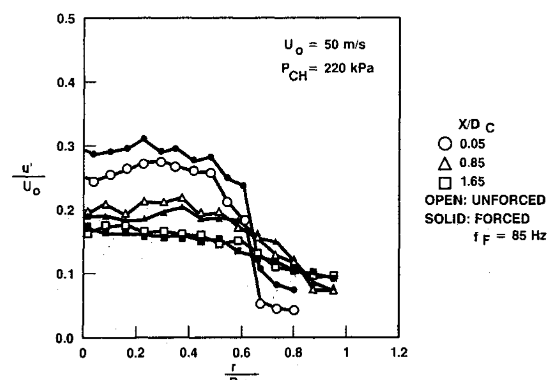

Fig. 9 Effect of forcing on ducted, multistep jet (turbulence intensity).

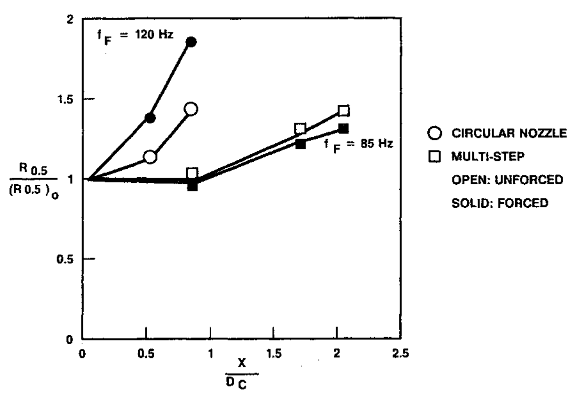

Fig. 10 Effect of forcing on the spread of ducted circular and multistep jets.

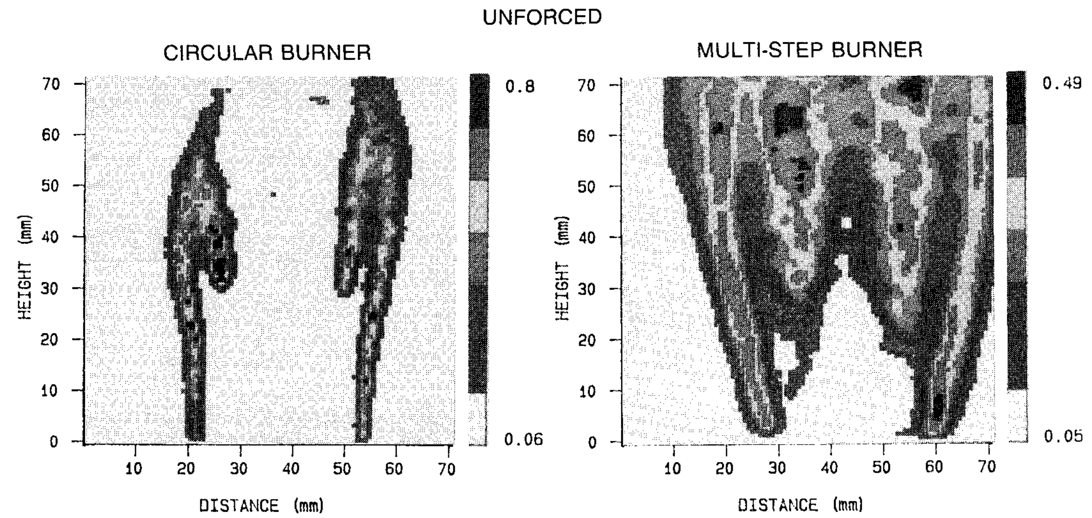

Fig. 11 Turbulence enhancement in diffusion flames with multistep burner.

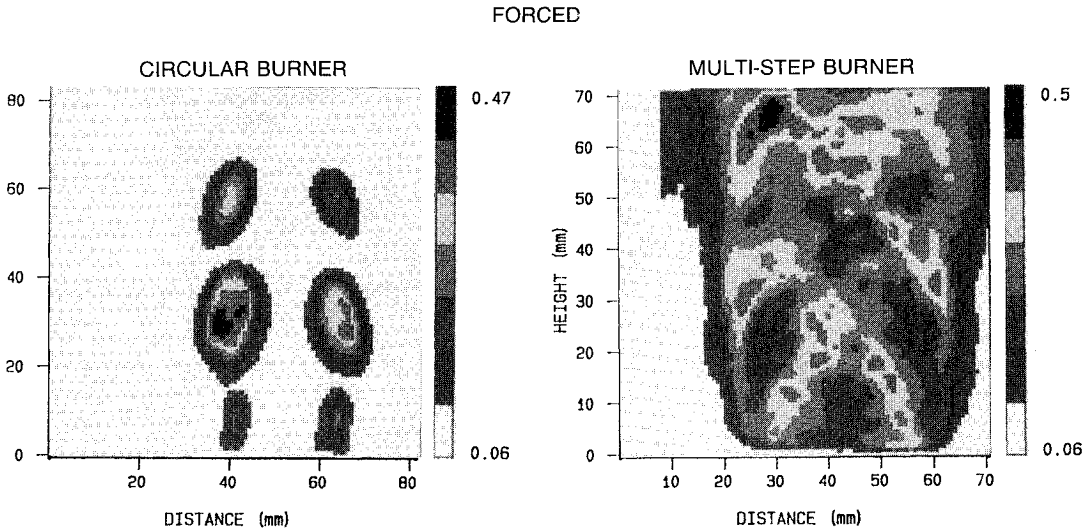

Fig. 12 Effect of forcing on circular and multistep diffusion flames.

the velocity-gradient decrease reduces the strain rate, the following test results show that the multistep arrangement produces many sources of fine-scale turbulence generation.

For the multistep nozzle, the resulting turbulence intensity at the exit was up to six times higher than that of a flow discharging from a regular circular nozzle (Fig. 6). Further tests showed that this turbulence intensity increase is associated with a substantial increase in fine-scale turbulence. Figure 7 shows the spectral distribution of the multistep jet as measured in the center of the nozzle's exit. This spectrum is compared with that of a circular jet measured at the same location. The turbulence intensity for the multistep nozzle is higher in the entire measured frequency range. The highest difference is for frequencies higher than 500 Hz. In this range, the multistep jet reaches peak values that are more than a decade higher than the circular jet. The multistep jet turbulence also exhibits a fully developed turbulence spectral distribution, containing an inertial subrange of $-5/3$ slope. The turbulent fluctuations associated with this subrange and those of higher frequencies are related to the fine-scale turbulence generated by this nozzle.

The difference of the shear-flow characteristics between both nozzles may also be seen from the forced-jet experiments. The circular jet has been studied before in detail using the same experimental arrangement.[13,14] A limited number of tests were made in the present study and will be discussed later to provide a direct comparison with the multistep nozzle. The earlier tests had shown that the highest response to forcing was achieved when the forcing Strouhal number matched the jet's preferred-mode Strouhal number, $St_j = f_j \times D/U_0 = 0.3$. The jet spread was enhanced through the generation or enhancement of large-scale structure.[13] The jet was also responsive to forcing when the forcing Strouhal number was decreased to $St = 0.03$.[14] This forcing also increased the jet spread and augmented the turbulence intensity through collective interaction.[6] The initial mean velocity profile was not affected by the forcing.

The multistep jet is very different in its response to forcing. Since the jet initial shear layer is much thicker, the growth rate of disturbance is reduced. It becomes difficult to excite large-scale structures in the thick shear layer, which has a high level of energetic fine-scale turbulence. Figures 8 and 9 demonstrate the nonresponsiveness of the multistep jet to forcing. Figure 8 depicts the unforced and forced jet at three axial locations. Figure 9 gives the turbulence intensity levels at the same stations under the same conditions. Both figures show that the jet mean and turbulent flowfields were not changed under forcing. The spreading rate did not increase, and the turbulence intensity was not augmented by forcing in contrast to the behavior of the circular jet.[13,14]

The spreading rate change due to forcing for the circular and multistep nozzles is compared in Fig. 10, using the jet's half-velocity radius $R_{0.5}$ (the radius of the jet where the mean velocity drops to half of its centerline value). With forcing, the width of the ducted circular jet grew by more than 35% in less than one duct diameter (D_{CH}) from the exit; without forcing, the spread of the multistep jet changed by less than 5% after 2 D_{CH}. The spreading rate of the multistep ducted jet was much lower than that of a circular ducted jet. The multistep jet spread by only 30% relative to its initial radius at $X = 2$ D_{CH}, whereas the circular jet spread by over 40% at half of the axial distance downstream of the nozzle.

Reacting Flow

Free Flame

The fine-scale turbulence-enhancement method using multiple steps, which was conceived and studied in nonreacting flows, was applied to combustion in free flames. The PLIF imaging technique was used to compare a regular circular burner flame to a multistep burner flame for both unforced and forced conditions. The averaged (5 s long) concentration of the hydroxyl radicals in the flame was used as an indicator of the combustion intensity. The combustion of the unforced circular flame was confined to the thin shear layer surrounding the jet (Fig. 11, left side). The unforced multistep flame was much more intense and uniformly spread throughout the jet (Fig. 11, right side). This difference can be attributed to the homogeneous distribution of high-intensity fine-scale turbulence in the multistep flame that enhances the combustion by promoting the molecular mixing of fuel and air. In the circular flame, these conditions exist only in the jet shear layer.

The forcing induced large-scale structures in the circular flame shear layer (Fig. 12, left side). The flame was enclosed in the large-scale structures where the required fine scale mixing conditions are available. The flame was quenched in the small streaks connecting the vortices (the "braids") due to the high strain rates in the flow at this region. The flame of the multistep nozzle was more homogeneously distributed without any trace of coherent structures (Fig. 12, right side). The fine-scale turbulence and reduced strain rates resulted in more uniform and stable flame characteristics. The lack of coherent structures during forcing illustrates the nonresponsiveness of the multistep jet flow to forcing.

Fuel-Rich Plume Combustion

The circular and multistep nozzles were compared in gas-generator tests to study the effect of fine-scale turbulence enhancement and reduced strain rates on the combustion intensity and stability of a high-velocity ducted fuel-rich plume in a high-pressure environment.

The plumes of the two nozzles were photographed using a high-speed movie camera operating at a speed of 400 frames/s. Still pictures were taken at a shutter speed of 1/200 s. The circular flame was detached (lifted off) from the gas-generator nozzle at $P_C = 500$ kPa. The detached flame was unstable with periodic reattachment of the flame at random circumferential locations (Fig. 13a). The detached flame was also bulged at the flame initial-ignition location. When the secondary-chamber pressure was reduced to 320 kPa, resulting in a higher plume velocity, the secondary-chamber flame could not be sustained.

The multistep nozzle changed the plume characteristics considerably. The flame was much more stable and was always attached to the nozzle. Even for the lowest secondary-chamber pressure tested (110 kPa), i.e., highest plume velocity, combustion was sustained in the secondary chamber without flame lift-off (Fig. 13b). The flame of the multistep nozzle was characterized by high turbulence with fine-scale activity that can be discerned especially at the flame edges.

The liftoff characteristics of the flame are related to the strain rates in the initial flow region, which may lead to local extinction when the strain exceeds a critical value.[4,5] The improved flame-holding characteristics of the multistep nozzle can be attributed to the reduction of the initial strain rate relative to a circular nozzle as a result of the change in the initial velocity profile that increased the initial shear-layer

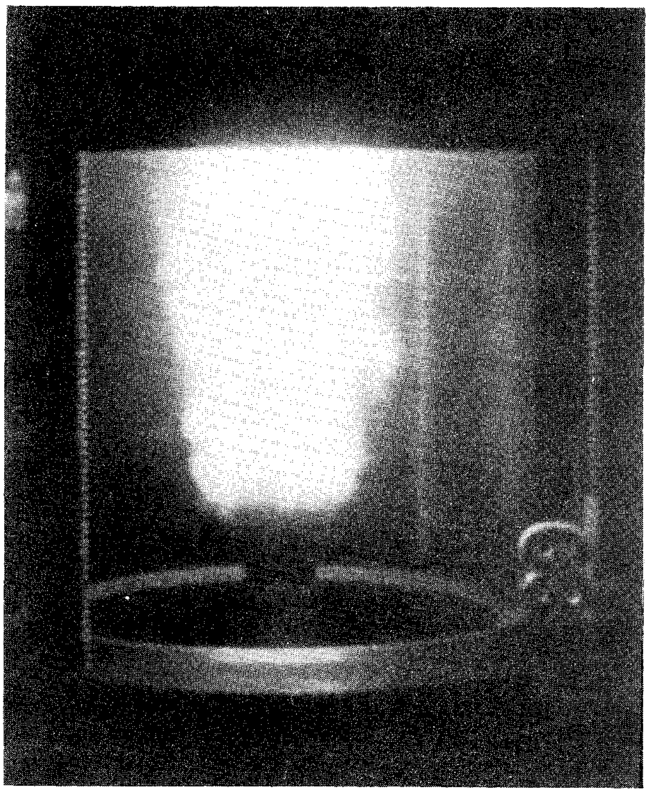

Fig. 13a Lifted-off flame of a circular nozzle in the secondary combustion chamber.

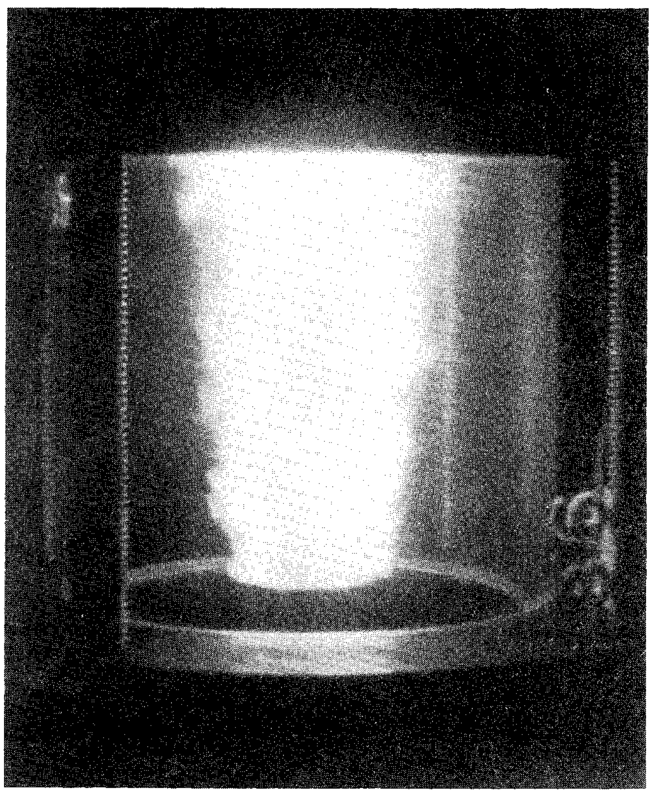

Fig. 13b Attached flame of a multistep nozzle in the secondary combustion chamber.

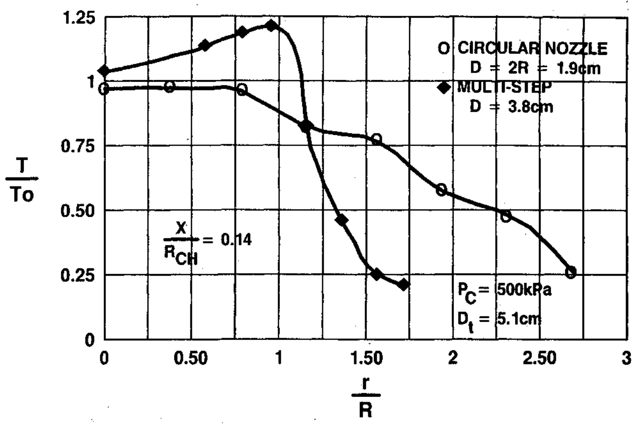

Fig. 14 Comparison of mean temperature profiles for circular and multistep gas-generator nozzles.

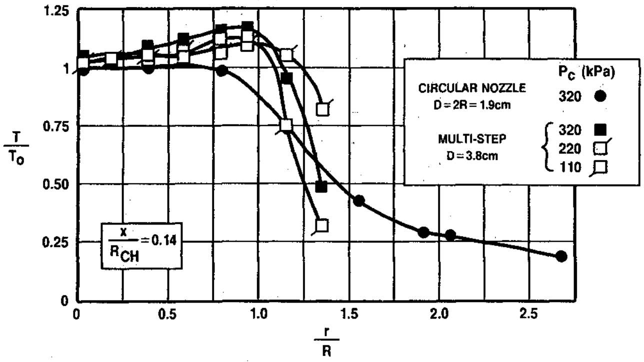

Fig. 15 Comparison of the mean temperature profiles for circular and multistep gas-generator nozzles at three combustor pressures.

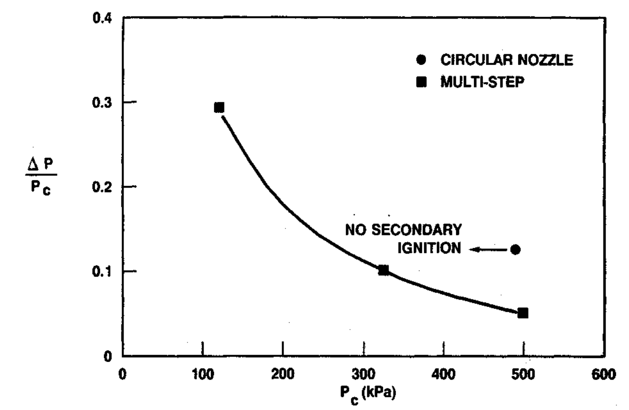

Fig. 16 Pressure oscillations amplitude variation with chamber pressure.

thickness, thus reducing the radial velocity gradients. In addition, the enhanced molecular mixing due to intense fine-scale turbulence has a stabilizing effect.

Temperature distribution in the plume measured by using a rake of eight thermocouples supported the observations made from the photographs. The mean temperature profiles shown in Fig. 14 were measured at the initial plume region at which the circular flame was still intermittently lifted off at $P_C = 500$ kPa. The center temperature was near that of the gas-generator combustor. The temperatures measured $r < 0.75\ R$ were averaged temperatures of intermittent flame excursions characteristic of the flame liftoff region. For the same P_C, the attached multistep flame had a temperature increase in the shear layer of nearly 25% relative to the gas-generator temperature due to plume afterburning in this region. When the secondary-chamber pressure was reduced and, consequently, the plume velocity was increased, the circular plume was even less stable and lifted off further away from the nozzle. At $P_C = 320$ kPa and lower pressure, the circular flame could not be sustained in the secondary chamber and the radial temperature distribution was typical for a heated jet mixing in a cooler coaxial stream (Fig. 15). At the same P_C, the multistep plume ignited. The multistep flame was stable with more than a 10% increase in the mixing layer temperature relative to the gas-generator temperature. A stable, attached flame was obtained with the multistep nozzle even with chamber pressures as low as $P_C = 110$ kPa, corresponding to supersonic plume-exit velocity.

The secondary-chamber pressure oscillations were measured for the two nozzles at the different chamber pressure conditions. At the highest pressure (Fig. 16), the circular flame combustion exhibited pressure oscillations that were more than two times higher than the multistep flame due to the flame instability. The amplitude of the pressure oscillations of the multistep flame did not increase for lower chamber pressures. No data are shown for the circular plume at the lower pressures because secondary ignition did not occur for these conditions.

The evolution of the two plumes along the secondary chamber was compared at the high chamber pressure conditions (Fig. 17). The circular plume that was initially detached ($X/D_{CH} = 0.07$) developed a mixing-layer-type temperature increase at $X/D_{CH} = 0.14$. The transition from an intermittent flame at the first cross section to a continuous flame at the second location was accompanied by a considerable increase in the plume's width. The third profile ($X/D_{CH} = 0.43$) had a nearly fully developed temperature distribution. The temperature increase relative to the gas generator was more than 25%. The multistep flame was attached to the nozzle. Therefore, the temperature profiles at all axial locations show increased temperature, also of more than 25%, in the shear-layer re-

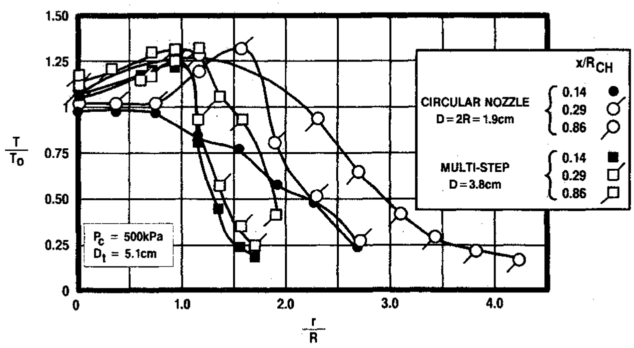

Fig. 17 Comparison of mean temperature profiles for circular and multistep gas-generator nozzles at three axial locations.

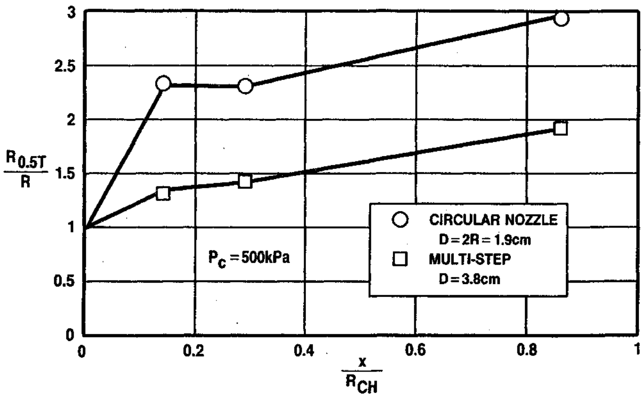

Fig. 18 Comparison of flame spread between circular and multistep gas-generator nozzles.

gion. The centerline temperatures of the multistep plume were larger than in the circular plume by nearly 10% due to the intense homogeneous small-scale mixing that characterizes this nozzle.

The spreading rates of the two plumes were similar, except for the large initial increase of the circular plume width at the location of ignition downstream of the lifted-off region (Fig. 18). The value of $R_{0.5T}$ (the radial distance where the temperature drops to half of its centerline value) at $X/D_{CH} = 0.07$ for the circular plume is an average distance that the intermittent unstable structures of the lifted flame are reaching.

Conclusions

An effective method of improving the combustion intensity and stability by enhancing fine-scale turbulence and reducing the strain rate in a fuel-rich plume was developed using basic knowledge of shear-flow dynamics. Initially, it was conjectured that the problem of flame lift-off and the absence of plume afterburning might be related to the lack of sufficient fine-scale turbulence in the initial shear layer of the flame. This lack is due to the dominance of large-scale structures that may also result in high strain rates at this region. Thus, different passive control methods were studied to enhance the fine-scale turbulence content in the flow at the nozzle exit and to reduce the strain rate. The multistep nozzle was able to accomplish both. The radial gradient in the initial mean velocity profile of the flame was reduced, resulting in lower strain rates. In addition, multiple inflection points were imposed on the mean flow, resulting in an increased number of instability sources. The fine-scale turbulence level was increased by a factor of six relative to a circular jet. The augmented fine-scale turbulence increased the molecular mixing of the combustion reactant, thus producing a homogeneous flame with high intensity. In addition, the reduced coherence of the flow structures at the nozzle exit eliminated the flame quenching due to high strain rates in the flow and, consequently, stabilized the flame. A stable flame was obtained with the multistep nozzle under the same conditions where afterburning was not achieved with the circular nozzle. The intensity of pressure oscillations in the secondary chamber was significantly lower with the multistep rather than circular nozzle.

Acknowledgments

The authors wish to thank Robert Smith for his help in performing the experiments.

References

[1]Abbot, S. W., Smoot, L. D., and Schadow, K. C., "Direct Mixing and Combustion Efficiency Measurements in Ducted, Particle-Laden Jets," *AIAA Journal*, Vol. 12, March 1974, pp. 275–282.

[2]Schadow, K. C., "Study of Gas-Phase Reactions in Particle-Laden, Ducted Flows," *AIAA Journal*, Vol. 11, July 1973, pp. 1042–1044.

[3]Schadow, K. C., "Fuel-Rich Particle-Laden Plume Combustion," *AIAA Journal*, Vol. 13, Dec. 1975, pp. 1553–1555.

[4]Kalghatgi, G. T., "Flow and Stability of Gaseous Jet Diffusion Flames," *Combustion Science and Technology*, Vol. 26, 1981, pp. 233–239.

[5]Peters, N. and Williams, F. A., "Lift-off Characteristics of Turbulent Jet Diffusion Flames," *AIAA Journal*, Vol. 21, 1983, pp. 423–429.

[6]Ho, C. M. and Huerre, P., "Perturbed Free Shear Layers," *Annual Review of Fluid Mechanics*, Vol. 16, 1984, pp. 365–426.

[7]Hussain, A. K. M. F., "Coherent Structures and Turbulence," *Journal of Fluid Mechanics*, Vol. 173, 1986, pp. 303–356.

[8]Schadow, K. C., Wilson, K. J., Lee, M. J., and Gutmark, E., "Enhancement of Mixing in Ducted Rockets With Elliptic Gas-Generator Nozzles," *Journal of Propulsion and Power*, Vol. 3, March-April 1987, pp. 145–149.

[9]Gutmark, E. and Ho, C. M., "Development of an Elliptical Jet," *Bulletin of the American Physical Society*, Vol. 27, 1982, p. 1184.

[10]Howard, L. N., "The Number of Unstable Modes in Hydrodynamic Instability Problems," *Journal De Mecanique*, Vol. 3, Dec. 1964, pp. 433–443.

[11]Kychakoff, G., Howe, R. D., Hanson, R. K., and McDaniel, J. C., "Quantitative Visualization of Combustion Species in a Plane," *Applied Optics*, Vol. 21, 1982, pp. 3225–3227.

[12]Parr, T., Gutmark, E., and Hanson-Parr, D., "Excimer Laser Induced Fluorescence Imaging System for OH Radicals in Flames," *Bulletin of the American Physical Society*, Vol. 31, 1986, p. 1680.

[13]Schadow, K. C., Gutmark, E., Wilson, K. J., Parr, D. M., Mahan, V. A., and Ferrell, G. B., "Effect of Shear-Flow Dynamics in Combustion Processes," *Combustion Science and Technology*, Vol. 54, 1987, pp. 103–116.

[14]Schadow, K. C., Wilson, K. J., Parr, D. M., and Gutmark, E., "Mixing Characteristics of a Ducted, Elliptical Jet With Dump," AIAA Paper 86-1399, June 1986.